

Adaptive Estimation of State of Charge for Lithium-ion Batteries

Fang, H.; Wang, Y.; Sahinoglu, Z.; Wada, T.; Hara, S.

TR2013-039 June 2013

Abstract

State of charge (SoC) estimation is a fundamental challenge in designing battery management systems. An adaptive SoC estimator, named as the AdaptSoC, is developed in this paper. It is able to estimate the SoC when the model parameters are unknown, through joint SoC and parameter estimation. Design of the AdaptSoC builds up on (1) a reduced complexity battery model that is developed from the well known single particle model (SPM) and, (2) joint local observability/identifiability analysis of the SoC and the unknown model parameters. Shown to be strongly observable, the SoC is estimated jointly with the parameters by the AdaptSoC using the iterated extended Kalman filter (IEKF). Simulation and experimental results exhibit the effectiveness of the AdaptSoC.

2013 American Control Conference (ACC)

This work may not be copied or reproduced in whole or in part for any commercial purpose. Permission to copy in whole or in part without payment of fee is granted for nonprofit educational and research purposes provided that all such whole or partial copies include the following: a notice that such copying is by permission of Mitsubishi Electric Research Laboratories, Inc.; an acknowledgment of the authors and individual contributions to the work; and all applicable portions of the copyright notice. Copying, reproduction, or republishing for any other purpose shall require a license with payment of fee to Mitsubishi Electric Research Laboratories, Inc. All rights reserved.

Adaptive Estimation of State of Charge for Lithium-ion Batteries

Huazhen Fang, Yebin Wang, Zafer Sahinoglu, Toshihiro Wada and Satoshi Hara

Abstract—State of charge (SoC) estimation is a fundamental challenge in designing battery management systems. An adaptive SoC estimator, named as the `AdaptSoC`, is developed in this paper. It is able to estimate the SoC when the model parameters are unknown, through joint SoC and parameter estimation. Design of the `AdaptSoC` builds up on (1) a reduced complexity battery model that is developed from the well-known single particle model (SPM) and, (2) joint local observability/identifiability analysis of the SoC and the unknown model parameters. Shown to be strongly observable, the SoC is estimated jointly with the parameters by the `AdaptSoC` using the iterated extended Kalman filter (IEKF). Simulation and experimental results exhibit the effectiveness of the `AdaptSoC`.

I. INTRODUCTION

In almost all Li^+ battery powered applications, state of charge (SoC) estimation plays a fundamental role in monitoring the battery status and regulating the charging and discharging processes for real-time battery protection and performance enhancement [1].

Literature review: SoC is the percentage ratio of the present battery capacity to the maximum capacity. Model-based SoC estimation has been given considerable attention in recent years, due to its incessant operation and improved accuracy. Equivalent circuit models (ECMs), which include virtual voltage source, internal resistance and RC network to simulate battery dynamics, have been used extensively. The state observability of a ECM is studied in [2], by which a SoC estimation algorithm is designed. In [3], the extended Kalman filter (EKF) is applied to ECMs to estimate the SoC. The estimation accuracy is enhanced in [4] using the sigma-point Kalman Filter (SPKF). Some other nonlinear observers have also been reported to construct ECM based SoC estimators, e.g., sliding mode observer [5], adaptive model reference observer [6] and Lyapunov-based observer [7].

Another important type of battery models are built upon electrochemical principles that describe the intercalation and diffusion of Li^+ ions and the conservation of charge within a battery. Such electrochemical models have the merit of ensuring each model parameter to retain a proper physical

meaning. However, their structure based on partial differential equations (PDEs) is complex. A linear reduced-order electrochemical model is established in [8], to which the classical KF is employed for SoC estimation. In [9], the EKF is implemented to estimate SoC via a nonlinear ordinary differential equation (ODE) model obtained from PDEs by finite-difference discretization. The unscented Kalman filter (UKF) is used in [10] to avoid model linearization for more accurate SoC estimation. Rather than using the ODE model after simplification, nonlinear SoC estimators are also developed in [11; 12] through direct manipulation of PDEs.

Adaptive SoC estimation, which enables the SoC to be estimated when the model parameters are unknown or vary with time, has been discussed for some ECMs and electrochemical models, e.g., [4; 13; 14]. This paper makes new contributions to study of this topic, with the aim of developing an adaptive SoC estimator that is theoretically sound and easy to implement.

Statement of contributions: An electrochemical model with reduced complexity in structure is obtained in the first place. For this model, a detailed analysis of joint local observability/identifiability of the SoC variable and the model parameters is performed. This attempt, despite its importance, has been rarely made in the literature on adaptive SoC estimation, to the author's best knowledge. The SoC variable is found to be able to be determined even though some model parameters are hardly identifiable. This indicates that adaptive estimation of at least the SoC is achievable. With the observability analysis, an adaptive SoC estimator, `AdaptSoC`, is built using the iterated extended Kalman filter (IEKF), where the SoC and model parameters are estimated concurrently but only SoC estimates are reliable.

II. A REDUCED-COMPLEXITY MODEL

In this section, the working mechanism of Li^+ batteries is briefly introduced first. Then a review of the single particle model (SPM) is presented, followed by appropriate model simplification for the purpose of SoC estimation.

A. The Working Mechanism of Li^+ Batteries

The structure of a Li^+ battery is schematically shown in Fig 1(a). The positive electrode is typically made from Li compounds, and the negative electrode usually contains graphite particles. Both have a porous structure, providing intercalation space such that the Li^+ ions can be moved in and out and stored. The electrolyte is electrically conductive so that the Li^+ ions can be transported easily. The separator separates the electrodes apart. It allows the exchange of Li^+ ions from one side to the other, but prevents electrons

H. Fang is with the Department of Mechanical and Aerospace Engineering, University of California, San Diego, CA 92093, USA, and currently visiting Mitsubishi Electric Research Laboratories, 201 Broadway, Cambridge, MA 02139, USA. hzfang@ucsd.edu

Y. Wang and Z. Sahinoglu are with Mitsubishi Electric Research Laboratories, 201 Broadway, Cambridge, MA 02139, USA. {yebingwang, zafer}@merl.com

T. Wada and S. Hara are with the Advanced Technology R&D Center, Mitsubishi Electric Corporation, 8-1-1, Tsukaguchi-honmachi, Amagasaki City, 661-8661, Japan. Wada.Toshihiro@bx.MitsubishiElectric.co.jp, Hara.Satoshi@cb.MitsubishiElectric.co.jp

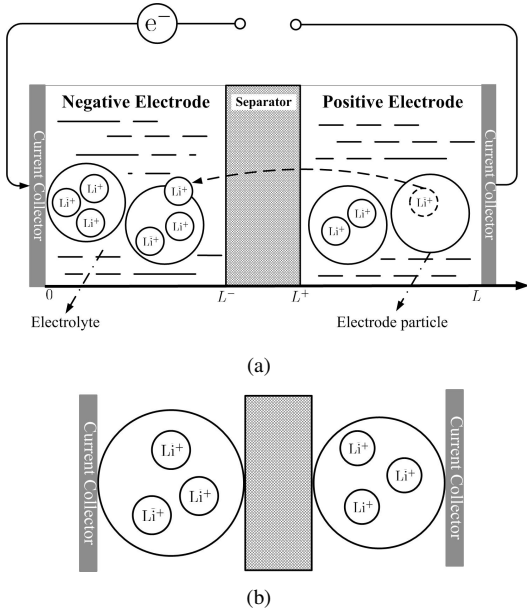


Fig. 1: (a) Schematic characterization of a Li^+ battery; (b) the single-particle model.

from passing through. The electrons are thus forced to flow through the external circuit.

During the charging process, Li^+ ions are extracted from the particles at the positive electrode into the electrolyte, and the particles at the negative electrode absorbs Li^+ ions from the electrolyte. This process not only generates an influx of Li^+ ions within the battery, but also builds up a potential difference between the positive and negative electrodes. In the reverse process the battery becomes discharged.

B. The Single Particle Model

The single particle model (SPM) (see Fig. 1(b)), as the name suggests, simplifies each electrode as a spherical particle with area equivalent to the active area of this electrode [15; 16]. It decreases complexities in identification, estimation and control design to a large extent [9; 12]. An introduction of the SPM is given below.

Input and output of the battery: The external input to the battery is the current $I(t)$ with $I(t) < 0$ for charge and $I(t) > 0$ for discharge. The terminal voltage is the potential difference between the two electrodes, that is,

$$V(t) = \Phi_{s,p}(t) - \Phi_{s,n}(t). \quad (1)$$

Conservation of Li^+ in the electrode phase: The migration of Li^+ ions inside a solid particle is caused by the gradient-induced diffusion. It follows from the Fick's laws of diffusion that

$$\frac{\partial c_{s,j}(r,t)}{\partial t} = \frac{1}{r^2} \frac{\partial}{\partial r} \left(D_{s,j} r^2 \frac{\partial c_{s,j}(r,t)}{\partial r} \right), \quad (2)$$

with the initial and boundary conditions given by

$$c_{s,j}(r,0) = c_s^0, \quad \left. \frac{\partial c_{s,j}}{\partial r} \right|_{r=0} = 0, \quad \left. \frac{\partial c_{s,j}}{\partial r} \right|_{r=\bar{r}_j} = -\frac{1}{D_{s,j}} J_j.$$

Variables

Φ_s	electric potential in the solid electrode
Φ_e	electric potential in the electrolyte
c_s	concentration of Li^+ in the solid electrode
c_{ss}	concentration of Li^+ at a particle's spherical surface
J	molar flux of Li^+ at the particle's surface
J_0	exchange current density
η	overpotential of reaction in the cell
U	open-circuit potential
I	external circuit current
V	terminal voltage
r	radial dimension of the particle

Physical parameters

D_s	diffusion coefficient of Li^+ in the solid electrode
\bar{r}	radius of the spherical particle
F	Farady's constant
S	specific interfacial area
T	temperature of the cell
α_a	anodic charge transport coefficient
α_c	cathodic charge transport coefficient
R	universal gas constant
R_c	phase resistance
R_f	film resistance of the solid electrolyte interphase

Subscripts

s	solid electrode phase
e	electrolyte phase
n	negative electrode
p	positive electrode
j	n or p

TABLE I: Definitions and nomenclature.

It is noted that J_j is the molar flux at the electrode/electrolyte interface of a single particle. When $j = n$ and p , respectively,

$$J_n(t) = \frac{I(t)}{FS_n}, \quad J_p(t) = -\frac{I(t)}{FS_p}.$$

Electrochemical kinetics: The molar flux J_j is governed by the Butler-Volmer equation:

$$J_j(t) = \frac{J_{0,j}}{F} \left[\exp\left(\frac{\alpha_a F}{RT} \eta_j(t)\right) - \exp\left(-\frac{\alpha_c F}{RT} \eta_j(t)\right) \right], \quad (3)$$

where

$$\eta_j(t) = \Phi_{s,j}(t) - \Phi_{e,j}(t) - U(c_{ss,j}(t)) - FR_{f,j}J_j(t).$$

The electrolyte phase can be represented by a resistor $R_{c,j}$ in the SPM, implying $\Phi_{e,j}$ can be expressed as $\Phi_{e,j}(t) = R_{c,j}I(t)$. Hence, η_j becomes

$$\eta_j(t) = \Phi_{s,j}(t) - U(c_{ss,j}(t)) - F\bar{R}_jJ_j(t), \quad (4)$$

where $\bar{R}_j = R_{c,j} + R_{f,j}$.

C. The Reduced Complexity Model

Average Li^+ concentration in the electrode phase: The average concentration of Li^+ ions in the particle is considered in the paper as the measure of the SoC. It is defined as

$$c_{s,j}^{\text{avg}}(t) = \frac{1}{\Omega} \int_{\Omega} c_{s,j}(r,t) d\Omega, \quad (5)$$

where Ω denotes the volume of the particle sphere. From (2), it is obtained that

$$\begin{aligned} \dot{c}_{s,j}^{\text{avg}}(t) &= \frac{1}{\Omega} \int_{\Omega} \frac{\partial c_{s,j}(r,t)}{\partial t} d\Omega \\ &= \epsilon_j D_{s,j} \left. \frac{\partial c_{s,j}(r,t)}{\partial r} \right|_{r=\bar{r}_j}, \end{aligned} \quad (6)$$

where ε_j is a constant coefficient. Depending on the electrode polarity, (6) splits into

$$c_{s,n}^{\text{avg}}(t) = -\frac{\varepsilon_n}{FS_n}I(t), \quad c_{s,p}^{\text{avg}}(t) = \frac{\varepsilon_p}{FS_p}I(t). \quad (7)$$

By (7), the rate of change of $c_{s,j}^{\text{avg}}$ is linearly proportional to the input current I . In other words, $c_{s,j}^{\text{avg}}$ is equal to the initial value $c_{s,j}^{\text{avg}}(0)$ plus integration of I over time. This illustrates that the change of SoC depends linearly on I as a result of $c_{s,j}^{\text{avg}}$ indicating SoC. Such a relationship has not only been presented for electrochemical models, e.g., [8], but has also been justified in ECMs, e.g., [3; 17] and the references therein.

Terminal voltage: Suppose there exists a function φ such that $c_{s,j}(t) = \varphi(c_{s,j}^{\text{avg}}(t))$ and define $\bar{U} = U \circ \varphi$, where ‘ \circ ’ denotes composition of two functions. Using (4), (1) becomes $V(t) = \bar{U}(c_{s,p}^{\text{avg}}(t)) - \bar{U}(c_{s,n}^{\text{avg}}(t)) + \eta_p(t) - \eta_n(t) + (\bar{R}_p - \bar{R}_n)I(t)$.

With $\alpha_a = \alpha_c = 0.5$, it follows from (3) that

$$\eta_n(t) = \frac{2RT}{F} \sinh^{-1} \left(\frac{J_n(t)F}{2J_{0,n}} \right) = \frac{2RT}{F} \sinh^{-1} \left(\frac{\varepsilon_n I(t)}{2J_{0,n}} \right),$$

$$\eta_p(t) = \frac{2RT}{F} \sinh^{-1} \left(\frac{J_p(t)F}{2J_{0,p}} \right) = \frac{2RT}{F} \sinh^{-1} \left(-\frac{\varepsilon_p I(t)}{2J_{0,p}} \right).$$

Thus $V(t)$ becomes

$$V(t) = \bar{U}(c_{s,p}^{\text{avg}}) - \bar{U}(c_{s,n}^{\text{avg}}) + \frac{2RT}{F} \left[\sinh^{-1} \left(-\frac{\varepsilon_p I(t)}{2J_{0,p}} \right) - \sinh^{-1} \left(\frac{\varepsilon_n I(t)}{2J_{0,n}} \right) \right] + (\bar{R}_p - \bar{R}_n)I(t). \quad (8)$$

As such, $V(t)$ consists of two parts. The first is the open-circuit voltage (OCV) that relies on $\bar{U}(c_{s,j}^{\text{avg}})$, and the second part is the direct feedthrough from I to V .

Construction of the state-space model: In above, (7)-(8) provide a concise characterization of the battery dynamics. To convert them into a state-space model for SoC estimation, denote the SoC by a state vector $x \in [0, 1]$. The input u and the output y of the model can be defined as $u = I$ and $y = V$, respectively. Since $c_{s,j}^{\text{avg}}$ is arguably equivalent to the SoC, the following is obtained from (7)-(8):

$$\begin{cases} \dot{x}(t) = -au(t), \\ y(t) = h(x(t)) + g(u(t)), \end{cases}$$

where a is a parameter, $h(\cdot)$ is the counterpart of the part containing \bar{U} in (8), and $g(\cdot)$ corresponds to the part involving I in (8). Discretization of the above system yields

$$\begin{cases} x_{k+1} = x_k - \alpha u_k, \\ y_k = h(x_k) + g(u_k), \end{cases} \quad (9)$$

where $\alpha = aT$ and T is the sampling period.

Note that, $h(\cdot)$ represents the SoC-OCV relationship and thus varies with different batteries. For the battery under consideration, it takes the parametric form as follows:

$$h(x) = \beta_0 \ln(x + \beta_1) + \beta_2.$$

In addition, $g(\cdot)$ can be determined from (8):

$$g(u) = \gamma_0 [\sinh^{-1}(\gamma_1 u) - \sinh^{-1}(\gamma_2 u)] + \gamma_3 u,$$

where γ_i for $i = 0, 1, 2, 3$ are parameters from (8).

Developed for SoC estimation, the model in (9) contains parameters α , β_i 's and γ_i 's. Their values are often hard to determine jointly and may even be subject to change over time. It is hence well worth considering ‘adaptive SoC estimation’ via simultaneous estimation of the SoC and the unknown parameters. A two-stage approach will be used:

- *Stage 1:* The parameters β_i 's in $h(\cdot)$ is determined using the SoC-OCV data set collected from experiments.
- *Stage 2:* After $h(\cdot)$ is obtained, the state $x(k)$, the parameters α and γ_i 's are estimated simultaneously.

This identification problem in Stage 1 can be formulated as a nonlinear least squares data fitting problem, which can be easily addressed by numerical methods such as the Gauss-Newton [18]. Therefore, β_i 's are assumed to be known in sequel. Indeed a nonlinear state and parameter estimation problem, Stage 2 is more complicated and will be the focus of the following study.

III. JOINT OBSERVABILITY/IDENTIFIABILITY ANALYSIS

Observability/identifiability analysis is crucial to state and parameter estimation. In this section, it is performed using the approach of sensitivity analysis.

Problem formulation: To study the joint observability/identifiability, the model in (9) is transformed into the model including the initial state and the parameters:

$$y_k = \phi(\theta; u_0, \dots, u_k), \quad (10)$$

where

$$\theta = [x_0 \quad \alpha \quad \gamma_0 \quad \gamma_1 \quad \gamma_2 \quad \gamma_3]^T,$$

$$\phi(\theta; u_0, \dots, u_k) = h \left(x_0 + \alpha \sum_{i=0}^{k-1} u_i \right) + g(u_k, \gamma).$$

In sequel, θ_i for $i = 1, 2, \dots, 6$ and its corresponding parameter will be used interchangeably. The identifiability problem for (10) is: Given the input data set $Z_N = \{u_0, \dots, u_N, y_0, \dots, y_N\}$, can θ be uniquely identified? If it cannot be, which parameters in θ can be determined with considerable accuracy?

Basics of sensitivity analysis: The sensitivity of y_k with respect to the change of θ is of interest. The sensitivity matrix for (10) is given by

$$S = \begin{bmatrix} \vdots & \vdots & \vdots & \vdots \\ s_{k1} & s_{k2} & \cdots & s_{k6} \\ \vdots & \vdots & \vdots & \vdots \end{bmatrix}, \quad (11)$$

where $s_{ki} = \partial y_k / \partial \theta_i$, for $i = 1, 2, \dots, 6$.

To estimate θ , consider the weighted mean-square-error cost function:

$$\ell(\theta) = \sum_{i=0}^N w_i \delta_i^2(\theta) = \Delta^T W \Delta,$$

where $w_i > 0$, $\delta_i = y_i - \phi(\theta; u_0, \dots, u_i)$, $\Delta = [\delta_0 \ \dots \ \delta_N]^T$, and $W = \text{diag}(w_0, \dots, w_N)$.

The best estimate of θ , denoted as θ^* , is the one that minimizes $\ell(\theta)$, that is,

$$\theta^* = \arg \min_{\theta} \ell(\theta).$$

It is known that θ^* will be the locally unique solution to minimize $\ell(\theta)$ if $\ell'(\theta^*) = 0$ and $\ell''(\theta^*) > 0$. Note that

$$\ell''(\theta) = 2S^T W S - 2 \sum_{i=0}^N \Delta^T W_i \frac{\partial}{\partial \theta} \left(\frac{\partial \phi(\theta; u_0, \dots, u_i)}{\partial \theta} \right)^T,$$

where W_i is the i -th column of W . When $\theta = \theta^*$, the second term in the right hand side becomes negligible because Δ approaches zero. Thus $\ell''(\theta^*)$ can be approximated as

$$\ell''(\theta) \approx 2S^T W S. \quad (12)$$

By (12), $\ell''(\theta^*) > 0$ if S has full column rank.

Local identifiability analysis of θ : For the battery model in (9), the sensitivity coefficients are given by

$$\begin{aligned} s_{k1} &= \frac{\beta_0}{x_0 + \alpha \sum_{i=0}^{k-1} u_i + \beta_1}, \quad s_{k2} = \frac{\beta_0 \sum_{i=0}^{k-1} u_i}{x_0 + \alpha \sum_{i=0}^{k-1} u_i + \beta_1}, \\ s_{k3} &= \sinh^{-1}(\gamma_1 u_k) - \sinh^{-1}(\gamma_2 u_k), \\ s_{k4} &= \frac{\gamma_0 u_k}{\sqrt{\gamma_1^2 u_k^2 + 1}}, \quad s_{k5} = -\frac{\gamma_0 u_k}{\sqrt{\gamma_2^2 u_k^2 + 1}}, \quad s_{k6} = u_k. \end{aligned}$$

The order of magnitude of each variable is: $x_0 \approx 10^{-1}$, $\alpha \approx 10^{-5}$, $\beta_0 \approx 10^0$, $\beta_1 \approx 10^0$, $\beta_2 \approx 10^0$, $\gamma_0 \approx 10^{-2}$, $\gamma_1 \approx -(10^{-7} \sim 10^{-6})$, $\gamma_2 \approx 10^{-7} \sim 10^{-6}$ and $\gamma_3 \approx 10^{-3} \sim 10^{-2}$. Suppose u_k lies within the reasonable range of $-20 \sim 20$.

Let s_{ki} be normalized to eliminate the scale-induced effects to fully show the influence of the change in θ_i on y_k :

$$s_{ki}^* = |\theta_i| s_{ki},$$

from which the normalized sensitivity matrix S^* can be defined accordingly. The normalized Hessian H^* is

$$\begin{aligned} H^*(\theta) &= \Gamma_{\theta} \ell''(\theta) \Gamma_{\theta} \\ &= S^{*T}(\theta) W S^*(\theta), \end{aligned}$$

where $\Gamma_{\theta} = \text{diag}(|\theta_1|, \dots, |\theta_6|)$. Analysis of s_{ki}^* and S^* establishes the following:

Fact 1: The parameter vector θ is almost locally unidentifiable.

Note that $s_{ki}^* \rightarrow 0$ for $i = 3, 4, 5$. This indicates that S_i^* for $i = 3, 4, 5$, where S_i^* is the i -th column of S^* , are almost linearly dependent. From a theoretical perspective, if $\{u_k\}$ contains a rich mix of frequency contents, S_2^* is independent of the other S_i^* 's. However, the order of magnitude of s_{k2}^* is quite small, which lies between $10^{-5} \sim 10^{-1}$, depending on the scale of $\{u_k\}$. It can be concluded that S^* will be almost surely rank-deficient in numerical sense, with rank of about 3. Thus θ can be hardly identified.

Even though θ cannot be identified, it is pointed out in [19] that a reparameterized model structure, or more specifically, a combination of parameters in θ , may be identified. The next remarkable fact is then established.

Fact 2: Despite Fact 1, x_0 can still be locally identified with high accuracy.

Intuitive thinking shows that x_0 can still be estimated due to the independence of S_1^* from S_i^* for $i = 2, \dots, 6$ and the order of magnitude of s_{k1}^* far exceeding s_{ki}^* for $i = 2, \dots, 6$. Consider the normalized Hessian H^* , which is rank deficient. Its singular value decomposition (SVD) can be expressed by

$$H^* = [U_l \ U_s] \begin{bmatrix} \Sigma_l & 0 \\ 0 & 0 \end{bmatrix} \begin{bmatrix} V_l^T \\ V_s^T \end{bmatrix}, \quad (13)$$

where U and V are unitary matrices and Σ_l is a diagonal matrix containing nonzero singular values of H^* . The rank of H^* is 3 since S^* has rank 3 as aforementioned. Hence, the dimensions of Σ_l , U_l and V_l are 3×3 , 6×3 and 6×3 , respectively. It can be proven that the column space of U_l is the subspace of the identifiable parameter space [19]. In other words, the vector ϑ obtained from reparameterizing θ is identifiable, where ϑ is given by

$$\vartheta = U_l^T \theta. \quad (14)$$

It is important to note that an element in ϑ will correspond to θ_1 or x_0 with extremely minor difference due to the numerical properties of S^* given above. That is, x_0 will be projected by U_l to a point in the identifiable subspace, which is very close to itself. Thus it can be identified with a considerable amount of accuracy.

From the above analysis, a joint state and parameter estimation algorithm can be designed, which, though only able to yield imprecise parameter estimates for α and γ_i 's, would still provide reliable state estimation results. Hence, adaptive SoC estimation will be achieved.

IV. ADAPTIVE SOC ESTIMATION

The adaptive SoC estimation is treated as joint state and parameter estimation addressed by an IEKF based technique. The IEKF is an improved version of the KF and EKF to deal with severe nonlinearities in the system by iteratively refining the state estimate around the current point at each time instant.

State augmentation: To use the IEKF, define an augmented state vector to incorporate both the original state x and the unknown parameters:

$$\xi_k = [x_k \ \alpha \ \gamma_0 \ \gamma_1 \ \gamma_2 \ \gamma_3]^T.$$

Thus (9) can be rewritten as

$$\begin{cases} \xi_{k+1} = F_k(u_k) \xi_k, \\ y_k = \bar{h}(\xi_k, u_k), \end{cases} \quad (15)$$

where

$$F_k(u_k) = \begin{bmatrix} 1 & u_k & & & & \\ & 1 & & & & \\ & & \ddots & & & \\ & & & & & 1 \end{bmatrix},$$

$$\begin{aligned} \bar{h}(\xi_k) &= \beta_0 \log(\xi_{1,k} + \beta_1) + \beta_2 \\ &+ \xi_{3,k} [\sinh^{-1}(\xi_{4,k} u_k) - \sinh^{-1}(\xi_{5,k} u_k)] + \xi_{6,k} u_k. \end{aligned}$$

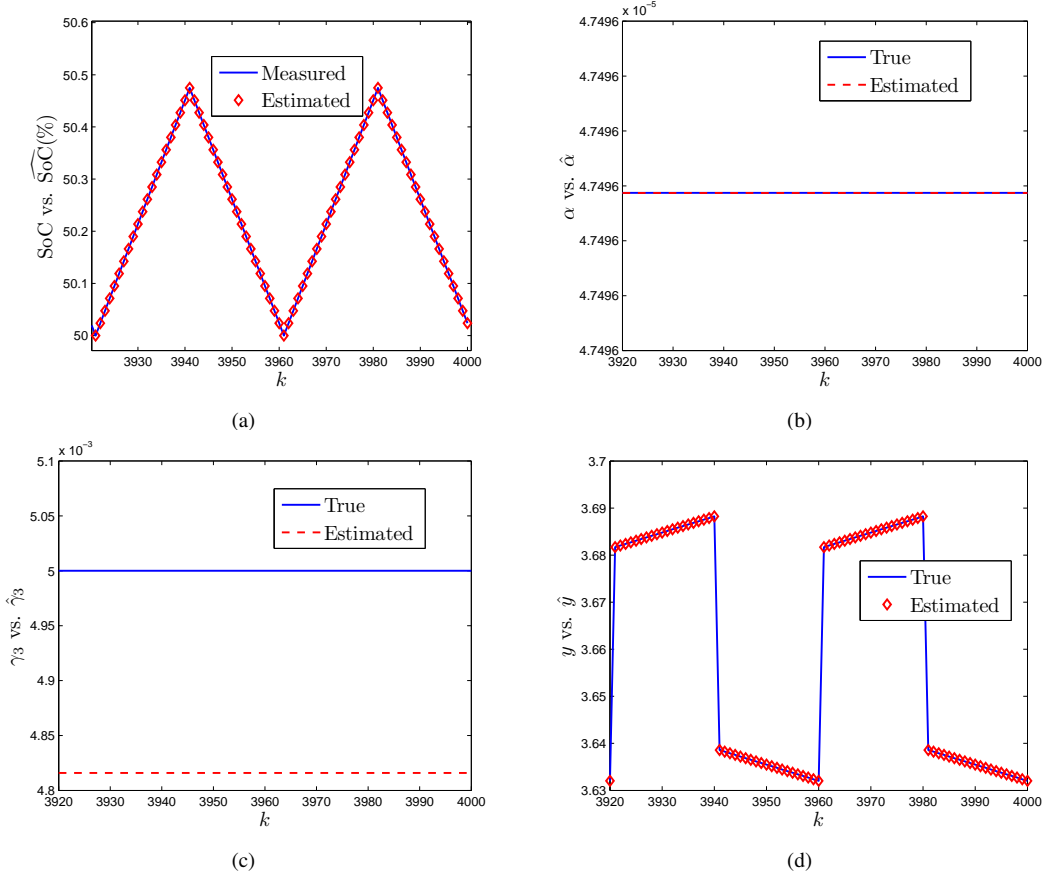


Fig. 2: Example 1 — noise-free case: (a) SoC estimation; (b) output estimation; (c) estimation of α ; (d) estimation of γ .

Application of IEKF: For the augmented battery model in (15), the IEKF is applied to estimating ξ_k . Like the KF and EKF, it consists of two procedures — prediction and update, which are implemented recursively.

The prediction formulae of the IEKF are

$$\hat{\xi}_{k|k-1} = F_{k-1}(u_{k-1})\hat{\xi}_{k-1|k-1}, \quad (16)$$

$$P_{k|k-1} = F_{k-1}(u_{k-1})P_{k-1|k-1}F_{k-1}^T(u_{k-1}) + Q, \quad (17)$$

where $\hat{\xi}_{k|k-1}$ and $\hat{\xi}_{k|k}$ are the estimates of ξ_k given Z_{k-1} and Z_k , respectively, P is the estimation error covariance, and $Q > 0$ is adjustable to reduce the effects of process noise.

The update is implemented iteratively:

$$K_k^{(i)} = P_{k|k-1}H_k^{(i-1)} \left[H_k^{(i-1)}P_{k|k-1}H_k^{(i-1)T} + R \right]^{-1}, \quad (18)$$

$$\hat{y}_k^{(i)} = \bar{h}(\hat{\xi}_{k|k}^{(i-1)}) - H_k^{(i-1)}(\hat{\xi}_{k|k-1} - \hat{\xi}_{k|k}^{(i-1)}), \quad (19)$$

$$\hat{\xi}_{k|k}^{(i)} = \hat{\xi}_{k|k-1} + K_k^{(i)}(y_k - \hat{y}_k^{(i)}), \quad (20)$$

where $R > 0$, the superscript (i) denotes the iteration number and

$$H_k^{(i)} = \left. \frac{\partial \bar{h}}{\partial \xi} \right|_{\hat{\xi}_{k|k}^{(i)}}.$$

The iteration process stops when i achieves the pre-specified maximum iteration number i_{\max} or when the error between two consecutive iterations is less than the pre-selected tolerance level. The associated estimation error covariance is

given by

$$P_{k|k} = (I - K_k^{(i_{\max})}H_k^{(i_{\max})})P_{k|k-1}. \quad (21)$$

The estimate of SoC is then given by $\hat{\xi}_{1,k}^{(i_{\max})}$.

The IEKF based adaptive SoC estimation algorithm, `AdaptSoC`, is summarized in (16)-(21). It has a recursive structure for sequential implementation, and furthermore, the update procedure is executed through iterative operations.

Essentially, the `AdaptSoC` is concerned with joint state and parameter estimation using state augmentation and the IEKF. Its development is motivated by conceptual simplicity, satisfying SoC estimation performance validated by experiments and modest computational complexity.

The update procedure of IEKF is equivalent to applying the Gauss-Newton method to finding the minimum of a mean-square-error cost function [20]. There are a few methods available in the literature as improvements of the Gauss-Newton method, e.g., the Levenberg-Marquardt algorithm. They can be used in the `AdaptSoC` to attain better estimation performance.

V. EXPERIMENTAL RESULTS

Two experiments are given to verify the findings and the effectiveness of the `AdaptSoC`. The first one is based on numerical simulation, and the second uses experimental data.

Experiment 1: Application of AdaptSoC to a perfect model. Consider the model in (9) and assume that it is

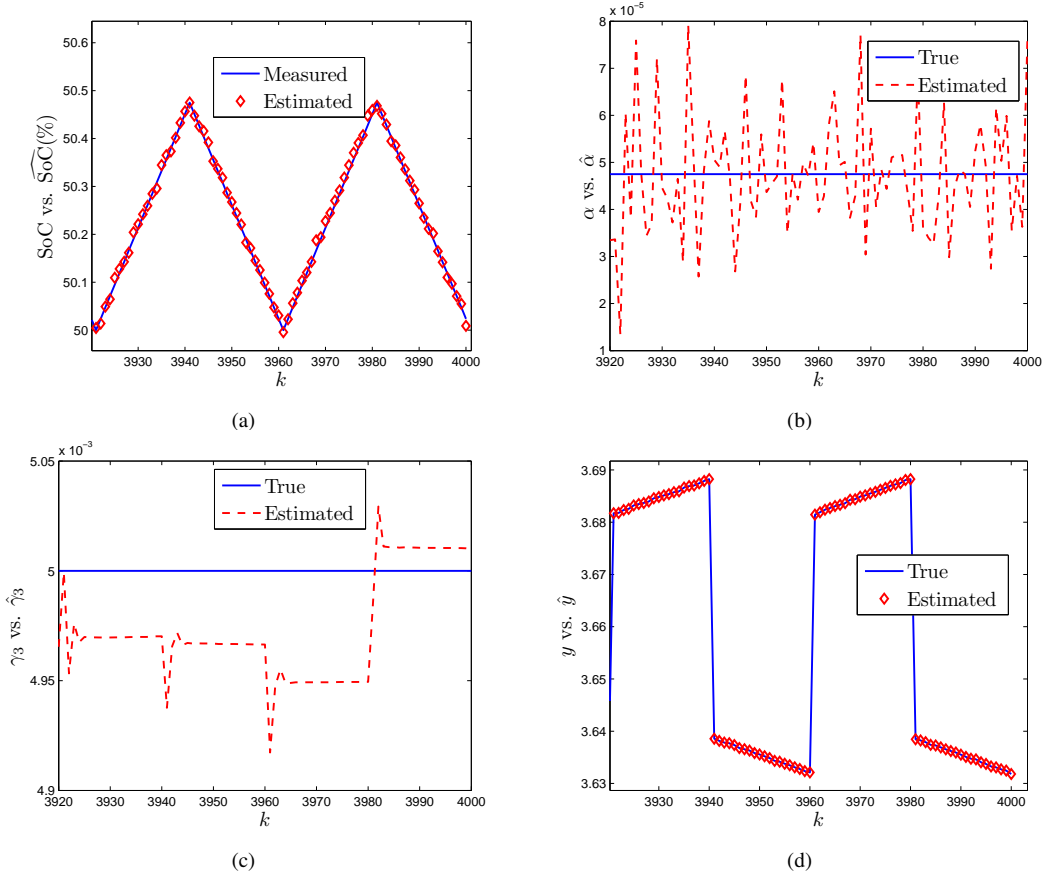


Fig. 3: Example 1 — noisy case: (a) SoC estimation; (b) output estimation; (c) estimation of α ; (d) estimation of γ .

accurate. The parameters are given as follows: $\alpha = 4.7496 \times 10^{-5}$, $\beta_0 = 1.0480$, $\beta_1 = 2.208 \times 10^{-1}$, $\beta_2 = 3.9998$, $\gamma_0 = 5.1400 \times 10^{-2}$, $\gamma_1 = 8.7615 \times 10^{-7}$, $\gamma_2 = -1.5274 \times 10^{-7}$, $\gamma_3 = -5 \times 10^{-3}$. The values of α and γ_i 's are reckoned according to [15; 16]. The values of β_i 's are determined by fitting the SoC-OCV data of the battery that will be experimented with in Example 3. The input to the model is a square wave alternating between 5 and -5 with period of 20s. Generate the simulation data using the model and then apply the *AdaptSoC*. The iteration number at each time step is set to be 10 in the update procedure.

The noise-free case is simulated first. The estimation results are shown in Fig. 2. It is shown in Figs. 2(a)-2(c) that the estimates of the SoC, α almost coincide with the true values. Yet estimation of γ_3 is not accurate. This observation supports the finding that the model parameter vector is not locally identifiable in Fact 1.

A weak noise with covariance of 10^{-8} is added to the measured output for further investigation. The estimation performance, as illustrated in Fig. 3, deteriorates as expected. Whereas estimation of α and γ_3 do not settle to fixed values, the SoC estimates are still satisfactory, validating Fact 2.

*Experiment 2: Application of *AdaptSoC* to experimental data.* The *AdaptSoC* is applied to data collected from practical experiments with a Li^+ battery. No details regarding the battery could be released at present due to required intellectual property protection. The SoC-OCV and current-

voltage data are obtained first. The values of β_i 's are identified from the SoC-OCV data at the first stage. Then the *AdaptSoC* is implemented to estimate the SoC during the second stage. The current applied is also a square wave alternating between 5A and -5 A with period of 10s. A rough estimate of the initial SoC is around 50%.

Fig. 4 summarizes the estimation results. From Fig. 4(a), it is seen that the SoC estimates change periodically as a result of the periodic input current, and that the range of variation is reasonable and as expected. Fig. 4(d) further shows the accurate output estimation through direct comparison with the truth. The parameter estimates of α and γ_3 shown in Figs. 4(b)-4(c) are obviously not convergent, indicating that the model does not fully match the true battery system. However, the SoC estimation even in this case is still considered reliable from the afore presented analysis and the subjective observation.

VI. CONCLUSION

Instead of following the design paradigm of ‘modeling—identification—SoC estimation’, this paper studies adaptive SoC estimation for Li^+ batteries, which integrates SoC estimation with parameter identification. A reduced complexity model is derived from the single particle model. Joint observability/identifiability of the SoC and the unknown parameters of the model is studied, showing the advantageous property that the SoC is strongly observable. An IEKF based adaptive

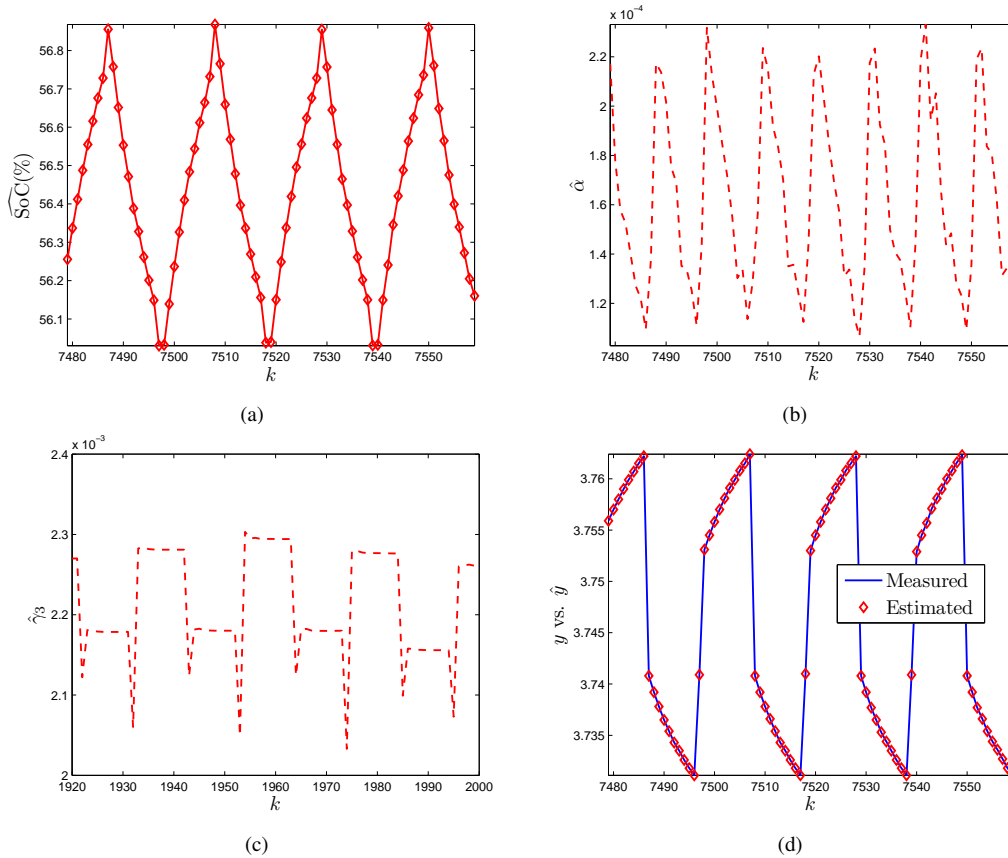


Fig. 4: Example 2: (a) SoC estimation; (b) output estimation; (c) estimation of α ; (d) estimation of γ_3 .

SoC estimator, the `AdaptSoC`, is then developed, which is also found to be noticeably robust against model mismatch. The analysis results and the performance of the `AdaptSoC` are verified by both simulation and practical experiments.

REFERENCES

- [1] N. Chaturvedi, R. Klein, J. Christensen, J. Ahmed, and A. Kojic, "Algorithms for advanced battery-management systems," *IEEE Control Systems Magazine*, vol. 30, no. 3, pp. 49–68, 2010.
- [2] J. Chiasson and B. Vairamohan, "Estimating the state of charge of a battery," *IEEE Transactions on Control Systems Technology*, vol. 13, no. 3, pp. 465–470, 2006.
- [3] G. L. Plett, "Extended Kalman filtering for battery management systems of LiPB-based HEV battery packs: Part 3. state and parameter estimation," *Journal of Power Sources*, vol. 134, no. 2, pp. 277–292, 2004.
- [4] —, "Sigma-point Kalman filtering for battery management systems of LiPB-based HEV battery packs: Part 2: Simultaneous state and parameter estimation," *Journal of Power Sources*, vol. 161, no. 2, pp. 1369–1384, 2006.
- [5] I.-S. Kim, "The novel state of charge estimation method for lithium battery using sliding mode observer," *Journal of Power Sources*, vol. 163, no. 1, pp. 584–590, 2006.
- [6] M. Verbrugge and E. Tate, "Adaptive state of charge algorithm for nickel metal hydride batteries including hysteresis phenomena," *Journal of Power Sources*, vol. 126, no. 1-2, pp. 236–249, 2004.
- [7] Y. Hu and S. Yurkovich, "Battery cell state-of-charge estimation using linear parameter varying system techniques," *Journal of Power Sources*, vol. 198, pp. 338–350, 2012.
- [8] K. A. Smith, C. D. Rahn, and C.-Y. Wang, "Model-based electrochemical estimation of lithium-ion batteries," in *Proc. IEEE International Conference on Control Applications*, 2008, pp. 714–719.
- [9] D. Domenico, G. Di Fiengo, and A. Stefanopoulou, "Lithium-ion battery state of charge estimation with a Kalman filter based on an electrochemical model," in *Proc. IEEE International Conference on Control Applications*, 2008, pp. 702–707.
- [10] S. Santhanagopalan and R. E. White, "State of charge estimation using an unscented filter for high power lithium ion cells," *International Journal of Energy Research*, vol. 34, no. 2, pp. 152–163, 2010.
- [11] R. Klein, N. A. Chaturvedi, J. Christensen, J. Ahmed, R. Findeisen, and A. Kojic, "Electrochemical model based observer design for a lithium-ion battery," *IEEE Transactions on Control Systems Technology*.
- [12] S. J. Moura, N. A. Chaturvedi, and M. Krstic, "PDE estimation techniques for advanced battery management systems - Part I: SOC estimation," in *Proc. American Control Conference*, 2012, pp. 559–565.
- [13] O. Barbarisi, F. Vasca, and L. Glielmo, "State of charge Kalman filter estimator for automotive batteries," *Control Engineering Practice*, vol. 14, no. 3, pp. 267–275, 2006.
- [14] M. McIntyre, T. Burg, D. Dawson, and B. Xian, "Adaptive state of charge (SOC) estimator for a battery," in *Proc. American Control Conference*, 2006, pp. 5740–5744.
- [15] S. Santhanagopalan, Q. Guo, P. Ramadass, and R. E. White, "Review of models for predicting the cycling performance of lithium ion batteries," *Journal of Power Sources*, vol. 156, no. 2, pp. 620–628, 2006.
- [16] M. Guo, G. Sikha, and R. E. White, "Single-particle model for a lithium-ion cell: Thermal behavior," *Journal of The Electrochemical Society*, vol. 158, no. 2, pp. A122–A132, 2011.
- [17] M. Coleman, C. K. Lee, C. Zhu, and W. G. Hurley, "State-of-Charge determination from EMF voltage estimation: Using impedance, terminal voltage, and current for lead-acid and lithium-ion batteries," *IEEE Transactions on Industrial Electronics*, vol. 54, no. 5, pp. 2550–2557, 2007.
- [18] G. A. F. Seber and C. J. Wild, *Nonlinear Regression*. Wiley, 2003.
- [19] J. F. Van Doren, S. G. Douma, P. M. Van den Hof, J. D. Jansen, and O. Bosgra, "Identifiability: From qualitative analysis to model structure approximation," in *Proc. 15th IFAC Symposium on System Identification*, 2009, pp. 664–669.
- [20] B. Bell, "The iterated Kalman filter update as a Gauss-Newton method," *IEEE Transactions on Automatic Control*, vol. 38, no. 2, pp. 294–297, 1993.